doi: 10.4149/gpb_2026024

Electroacupuncture alleviates synovial inflammation in rheumatoid arthritis rats by suppressing caspase-1-mediated pyroptosis

Xiling Chen[1,*], Kui Fang[1,*], Peng Xu[1], Xiaojing Nan[1], Jinbiao You[1], Yingjun Xiao[1] and Zheqing Dong[1]

[1] *Clinical Laboratory, The Third Affiliated Hospital of Zhejiang Chinese Medical University, Hangzhou, China*

Abstract. Rheumatoid arthritis (RA) causes inflammatory bone and cartilage damage. While electroacupuncture (EA) alleviates joint inflammation, its anti-inflammatory mechanisms remain unclear. Sprague-Dawley rats were randomly assigned to control, collagen-induced arthritis (CIA), EA (EA+CIA), and sham-EA (sham-EA+CIA) groups. Rats in the EA group received EA at unilateral ST36 (Zusanli) every other day from day 1. Paw swelling and paw withdrawal latency (PWL) were measured during the treatment. The levels of caspase-1, GSDMD, IL-1β, and IL-18 in the synovium were assessed after 28 days of EA treatment. Our findings demonstrated that inflammatory responses, such as the arthritis index, toe volume, PWL, and inflammatory cell infiltration, were significantly improved in the EA group compared with the CIA and sham-EA groups. Significant decreases in the levels of caspase-1, GSDMD, IL-1β, and IL-18 were observed in the synovium of RA rats that received EA. Furthermore, peripheral blood levels of the inflammatory cytokines IL-1β and IL-18 were significantly reduced in rats in the EA group. Electroacupuncture as implemented at ST36 was associated with reduced caspase-1-mediated pyroptosis-related markers in the joint synovium and decreased IL-1β and IL-18 levels in both synovium and serum in rats with CIA. Acupoint-specificity requires further validation using active-sham or component-resolved control designs.

Key words: Electroacupuncture — Rheumatoid arthritis — Pyroptosis — Gasdermin D

Abbreviations: BCA, bicinchoninic acid; CFA, complete Freund's adjuvant; CIA, collagen-induced arthritis; DMARDs, disease-modifying anti-rheumatic drugs; EA, electroacupuncture; ELISA, enzyme-linked immunosorbent assay; IFA, incomplete Freund's adjuvant; PWL, paw withdrawal latency; RA, rheumatoid arthritis.

Introduction

Rheumatoid arthritis (RA) is a chronic inflammatory disease that can cause significant damage to bone and cartilage, potentially leading to disability. While several treatments are available, including disease-modifying anti-rheumatic drugs (DMARDs) and glucocorticoids, these medications often have undesirable side effects (Chauhan 2023). Acupuncture, a traditional Chinese medicine practice, is a promising treatment for RA patients that can alleviate joint inflammation without reported side effects. EA, a variation of acupuncture, uses pulsed currents applied to specific acupoints on the body. Although EA has demonstrated clinical efficacy, the mechanisms by which it affects RA patients are not yet fully understood (Lu 2022; Wan et al. 2022).

* These authors contributed equally to this work.
Correspondence to: Zheqing Dong, Clinical Laboratory, The Third Affiliated Hospital of Zhejiang Chinese Medical University, Hangzhou, China
E-mail: dongzqzsyy@outlook.com

Programmed cell death (PCD) has been widely studied and verified to be one of the essential pathological mechanisms of RA (Zhao 2021). Pyroptosis is a type of proinflammatory PCD and is mainly initiated by caspase activation. The canonical pyroptosis pathway is activated by caspase-1 activation followed by cleavage of downstream proteins, such as gasdermin D (GSDMD), IL-1β, and IL-18. The N-terminal fragment of GSDMD (N-GSDMD) generates pyroptotic pores on the cell membrane, which promote proinflammatory cytokine release, resulting in joint inflammation and tissue damage (Shi 2017). Caspase-1/GSDMD is an important downstream pathway of various mediators of cell pyroptosis, such as the NLRP3 inflammasome, that participate in numerous immune regulation processes. Caspase-1-mediated pyroptosis is detected in RA patients, as well as collagen-induced arthritis (CIA) mice (Guo et al. 2018; Zhou et al. 2021). Inhibiting GSDMD expression in arthritis mouse models reduces articular cartilage loss and inflammatory responses, highlighting caspase-1-mediated pyroptosis as an effective therapeutic target for treating RA (Yang et al. 2021). Recent evidence has shown that EA at ST36 negatively affects caspase-1-mediated pyroptosis in nervous system (Cai et al. 2022; Li et al. 2023), but the relationship between pyroptosis and EA in RA has not been studied.

This study aimed to investigate the mechanisms by which EA affects CIA rats, focusing on pyroptosis by measuring the protein levels of GSDMD, caspase-1, IL-1β, and IL-18 in the joint synovium. Additionally, the effects of EA on RA's inflammatory progression were evaluated by assessing the arthritis index, paw swelling, paw withdrawal latency (PWL), histological morphology, and serum cytokines. The findings of this study could enhance the understanding of EA's anti-inflammatory mechanisms in RA and potentially lead to the development of new therapeutic strategies for the disease.

Materials and Methods

Experimental animals

A total of 20 Sprague-Dawley rats (220–270 g, male, 6 to 8 weeks old) were obtained from The Zhejiang Chinese Medical University (ZCMU, Zhejiang, China) and were acclimatized for 1 week before the experiment. The rats were randomly divided into four groups ($n = 5$ *per* group) as follows: the control group, the CIA group, the EA group (EA+CIA), and the sham-EA group (sham-EA+CIA). The rats were maintained at a temperature of 24 ± 1°C and subjected to a light/dark cycle with free access to food and water. All experimental procedures were approved by the laboratory animal management and ethics committee of ZCMU (Approval ID: IACUC-20220505-05).

RA model establishment

Briefly, rats were injected intradermally with 0.5 ml of bovine collagen type II (1 mg/ml) in complete Freund's adjuvant (CFA) at the intraplantar and base of the tail on day 0. On day 14, a half dose of collagen type II in incomplete Freund's adjuvant (IFA) was injected after inflammatory evaluations as a booster. The control group received an equal amount of saline injected into the same region.

EA

Before treatment, a soft cotton hood was placed over the rat's head to reduce stress. A disposable acupuncture needle (0.16 mm in diameter; Hwato, Suzhou, China) was inserted vertically to a depth of 5 mm at ST36 on one hindlimb (located 3–4 mm below and 1–2 mm lateral to the knee midline). Electrical stimulation was delivered using an electroacupuncture apparatus (SDZ-II; Hwato Medical Electronic Apparatus, Suzhou, China). The cathode (negative lead) was connected to the needle, and the anode (positive lead) was attached to the plantar surface of the ipsilateral hindlimb with wet gauze as the return electrode. Stimulation was applied in continuous mode (fixed frequency, no dense–disperse modulation) at 20 Hz and 1 mA for 30 min, using an asymmetric biphasic pulsed waveform (composite waveform; non-sinusoidal) (Xue et al. 2023). EA was administered once every other day starting on day 1 (alternating hindlimbs each time).

In the sham-EA group, a needle was inserted subcutaneously to a depth of 2 mm at a non-acupoint approximately 5 mm lateral to ST36, with electrodes attached in the same manner but without electrical current (Xue et al. 2023). The non-acupoint site was selected by avoiding recognized acupoints according to the Animal Acupuncture Atlas (Experimental Acupuncture Research Group of the Chinese Acupuncture Association). The sham-EA procedure was designed as a minimal-activation procedural control to account for handling and superficial skin penetration while minimizing deep-tissue stimulation and electrostimulation; therefore, it differed from EA in needling depth, anatomical location, and electrical current by design and should not be interpreted as an active-sham intended to isolate site specificity.

The ST36 (Zusanli) region in rats was localized with reference to the Animal Acupuncture Atlas and standardized using consistent anatomical landmarks of the hindlimb. To minimize inter-operator variability, all localization and needling procedures were performed by a single experienced practitioner throughout the study, with a standardized hindlimb posture and insertion angle. The sham site was defined as a non-acupoint located approximately 5 mm lateral to the ST36 region on the same hindlimb segment.

We acknowledge that rodent acupoint localization has inherent spatial uncertainty and that a 5-mm surface separation may not fully exclude overlap of underlying receptive fields; therefore, in this study the sham-EA procedure was designed as a minimal-activation control (shallow insertion without electrical current) rather than an active-sham intended to isolate site specificity.

Arthritis scoring

The arthritis index was calculated based on the degree of redness and swelling of the bilateral hindlimbs of the rat and whether normal function was affected. The arthritis score was evaluated based on the following scoring system (Xue 2020): 0, no signs of redness and swelling; 1, mild swelling or erythema of the toes; 2, redness or erythema in the toe joints and back of the foot and involving the ankle joint; 3, severe redness and swelling of the foot and ankle joints; and 4, serious redness and swelling of the foot and ankle joints and inability to bear weight, affecting normal exercise. The measurements were performed on day 1, day 7, day 14, day 21, and day 28.

Measurement of nociceptive thresholds and paw swelling

Paw swelling was evaluated by using a water displacement method and a toe volume measuring instrument (KW-7C, Calvin Biotechnology Co., Nanjing, China). PWL was evaluated as a nociceptive threshold indicator using a ZL-024D heat pain stimulation instrument (Yaokun Biotechnology Co., Anhui, China). The method of PWL measurement was described in Wang et al. (2014). Before testing, the rats were allowed to acclimatize to the environment for 30 min. The heat was adjusted to obtain PWLs within 20–25 s in normal paws (on day −1). Then, the plantar surface of the right paw was exposed to heat, and the PWL time was recorded. The time until paw withdrawal was used as the thermal nociceptive threshold. The PWL of the right hind paw was measured 3 times every 5 min, and the mean value was calculated and recorded. The measurement time points of PWL and paw swelling were the same as those used for arthritis scoring.

Serum cytokine detection

Serum IL-1β and IL-18 levels were detected by enzyme-linked immunosorbent assay (ELISA). Rat IL-1β and IL-18 ELISA kits were purchased from Nanjing Jiancheng Bioengineering Institute, China. The rats were euthanized by exposure to 100% CO_2 for 10 min. Synovial tissue of the knee joint was retrieved after pumping out cardiac blood on day 28. The tissue samples were stored in liquid nitrogen, and the blood samples were centrifuged at 2500×*g* for 10 min to extract serum. The levels of IL-1β and IL-18 were measured according to the manufacturer's instructions.

Hematoxylin and eosin (HE) staining of the rat synovium

Rat synovial tissue was obtained from the knee joints of rat hind legs as described in Hyc et al. (2007). The synovial tissues ($n = 5$ per group) were immersed in 4% formaldehyde overnight and then decalcified in 5% nitric acid solution for 1–3 days. Paraffin sections (5 μm thick) were rehydrated in a graded ethanol series and subjected to HE staining. The histological changes in the synovium of rats in each group were observed under a microscope.

Western blot

The joint synovial tissues ($n = 5$ *per* group) were preserved in liquid nitrogen, pulverized and dissolved in cell lysis buffer (Kaiji Biology, Jiangsu, China) containing a protease inhibitor cocktail (1%; Kaiji Biology, Jiangsu, China) and centrifuged at 12000×*g* for 10 min at 4°C for protein extraction. Protein concentrations were measured by the bicinchoninic acid (BCA) method. Primary polyclonal antibodies against GSDMD (Novus Biologicals, 1:40), Caspase-1 (Novus Biologicals, 1:40), IL-1β (Abcam, 1:26), IL-18 (Detroit R&D, 1:20), and GAPDH (Abcam, 1:200) were mixed with antibody diluent II (ProteinSimple, USA). Target proteins were then measured and imaged using the Wes automated protein expression analysis system, original auxiliary reagents, and the original secondary antibody (ProteinSimple, USA).

Statistical analysis

Data are presented as mean ± SD ($n = 5$ for each group). Statistical analyses were performed using SPSS 26. The arthritis index was analyzed by two-way repeated-measures ANOVA with Group (4 levels) as the between-subject factor and time (Day 1, 7, 14, 21, and 28) as the within-subject factor. When significant effects were detected, post hoc comparisons were performed using Tukey's test for between-group differences at each time point. A two-sided $p < 0.05$ was considered statistically significant.

Results

EA alleviates the inflammatory responses of CIA rats

The experimental design and workflow are depicted in Figure 1A. After modelling (day1), the degree of paw swelling in the model, EA, and sham-EA groups was significantly increased compared with the normal group ($p < 0.01$, Fig. 1B), while the PWL in the CIA, EA, and sham-EA groups was markedly

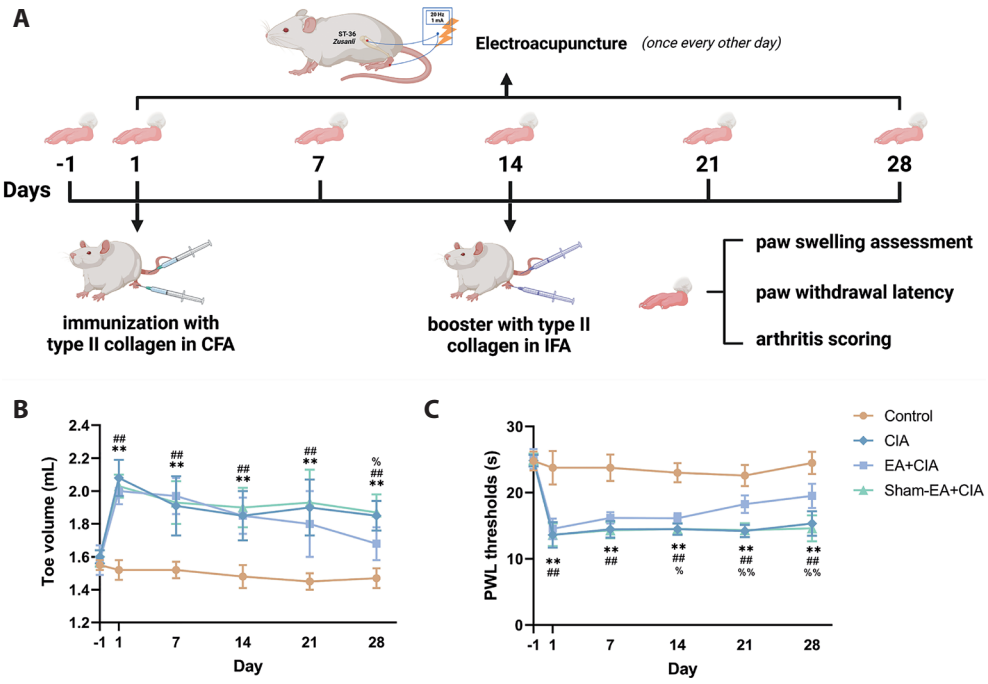

Figure 1. Toe volume and paw withdrawal latency (PWL) during the experimental period. **A.** Schematic overview of the collagen-induced arthritis (CIA) model and the electroacupuncture (EA) intervention schedule. **B.** Toe volume measured at the indicated time points in each group. **C.** Paw withdrawal latency (PWL) measured at the indicated time points in each group. Data are presented as mean ± SD. Statistical significance is indicated as follows: $^{\#}p < 0.05$ and $^{\#\#}p < 0.01$, CIA *vs.* control; $^{*}p < 0.05$ and $^{**}p < 0.01$, sham-EA+CIA *vs.* control; $^{\%}p < 0.05$ and $^{\%\%}p < 0.01$, EA+CIA *vs.* control.

decreased compared with the control group ($p < 0.01$, Fig. 1C), indicating that the Freund's adjuvant RA rat model had been successfully established.

After 14 days of treatment, there was no significant difference in paw swelling between the EA and CIA/sham-EA groups ($p > 0.05$, Fig. 1B); however, the PWL of the EA group was markedly improved compared with that of the model and sham-EA groups ($p < 0.05$, Fig. 1C). After 28 days of treatment, paw swelling in the EA group was significantly decreased compared with both the model and sham-EA groups ($p < 0.05$, Fig. 1B), while the PWL of the EA group was further elevated compared with both the model and sham-EA groups ($p < 0.01$, Fig. 1C).

The arthritis index increased markedly after CIA induction in the CIA, EA+CIA, and sham-EA+CIA groups, whereas the control group remained at 0 throughout the observation period. Repeated-measures ANOVA demonstrated significant main effects of Group and Time, as well as a significant Group×Time interaction (all $p < 0.001$), indicating that arthritis severity changed over time differently among groups. Compared with the CIA group, the EA+CIA group showed a significantly lower arthritis index at later time points, with the most evident reduction observed on Days 21 and 28 ($p < 0.05$ at the corresponding time points). In contrast, the sham-EA+CIA group did not show a sustained improvement relative to the CIA group, and its arthritis index remained comparable to that of the CIA group across most time points (Table 1).

Histopathological observation showed that there was no inflammatory cell infiltration in the synovial membrane

Table 1. The arthritis index in each group

Time	Control	CIA	EA+CIA	sham-EA+CIA	F (df)	*p*	ηp^2
Day −1	0	0	0	0			
Day 1	0	7.57 ± 0.28	7.57 ± 0.28	7.71 ± 0.24			
Day 7	0	7.28 ± 0.23	7.29 ± 0.57	7.14 ± 0.14			
Day 14	0	6.85 ± 0.47	6.85 ± 0.47	7.00 ± 0.33			
Day 21	0	7.28 ± 0.57	6.14 ± 0.47	7.42 ± 0.28			
Day 28	0	6.28 ± 0.23	4.85 ± 0.47	6.42 ± 0.28			
RM-ANOVA (Group)					8.171 (3, 16)	<0.001	0.476
RM-ANOVA (Time)					7.728 (4, 64)	<0.001	0.244
RM-ANOVA Group×Time)					7.136(12, 64)	<0.001	0.471

Data are means ± SD.

in the normal control group, but obvious infiltration of inflammatory cells and proliferation of synovial cells were observed in the model and sham-EA groups. Compared with the model and sham-EA groups, inflammatory cell infiltration was attenuated in RA rats treated with EA (Fig. 2). These findings suggest that EA at ST36 has a significant inhibitory effect on inflammatory responses in CIA rats.

EA suppresses caspase-1-mediated pyroptosis of the joint synovium

To elucidate the mechanism of the anti-inflammatory effect induced by EA, we investigated the expression of pyroptosis-related molecules in the synovium of the joint, including GSDMD (N-GSDMD, 36 kDa), caspase-1, pro-caspase-1, IL-1β, pro-IL-1β, IL-18, and pro-IL-18. As shown in Figure 3, activated caspase-1, GSDMD, and the activated proinflammatory cytokines IL-1β and IL-18 were significantly upregulated in the CIA and sham-EA groups compared with the control group ($p < 0.01$, Fig. 3A–E). The levels of activated caspase-1 and GSDMD in the EA group were significantly lower than those in the CIA and sham-EA groups ($p < 0.01$, Fig. 3A–C), as well as activated IL-1β and IL-18 ($p < 0.05$, Fig. 3A–E). These results demonstrated that EA treatment had negative effects on caspase-1-mediated pyroptosis and the proinflammatory factors IL-1β and IL-18 in the joint synovium.

EA reduces elevated serum pro-inflammatory cytokine levels in CIA rats

In the clinic, rheumatoid arthritis may impact organs other than the joint due to elevated levels of proinflammatory cytokines in serum. To study the effects of EA on serum cytokines, IL-1β and IL-18, which are strongly associated with RA, were investigated in each group. On day 28, the serum levels of IL-1β and IL-18 in the CIA and sham-EA groups were significantly higher than those in the control group ($p < 0.01$, Fig. 4A,B), and these two cytokines were significantly lower in the EA group than CIA and sham-EA groups ($p < 0.05$, Fig. 4A,B), indicating that EA treatment had a negative effect on serum proinflammatory cytokines in RA rats.

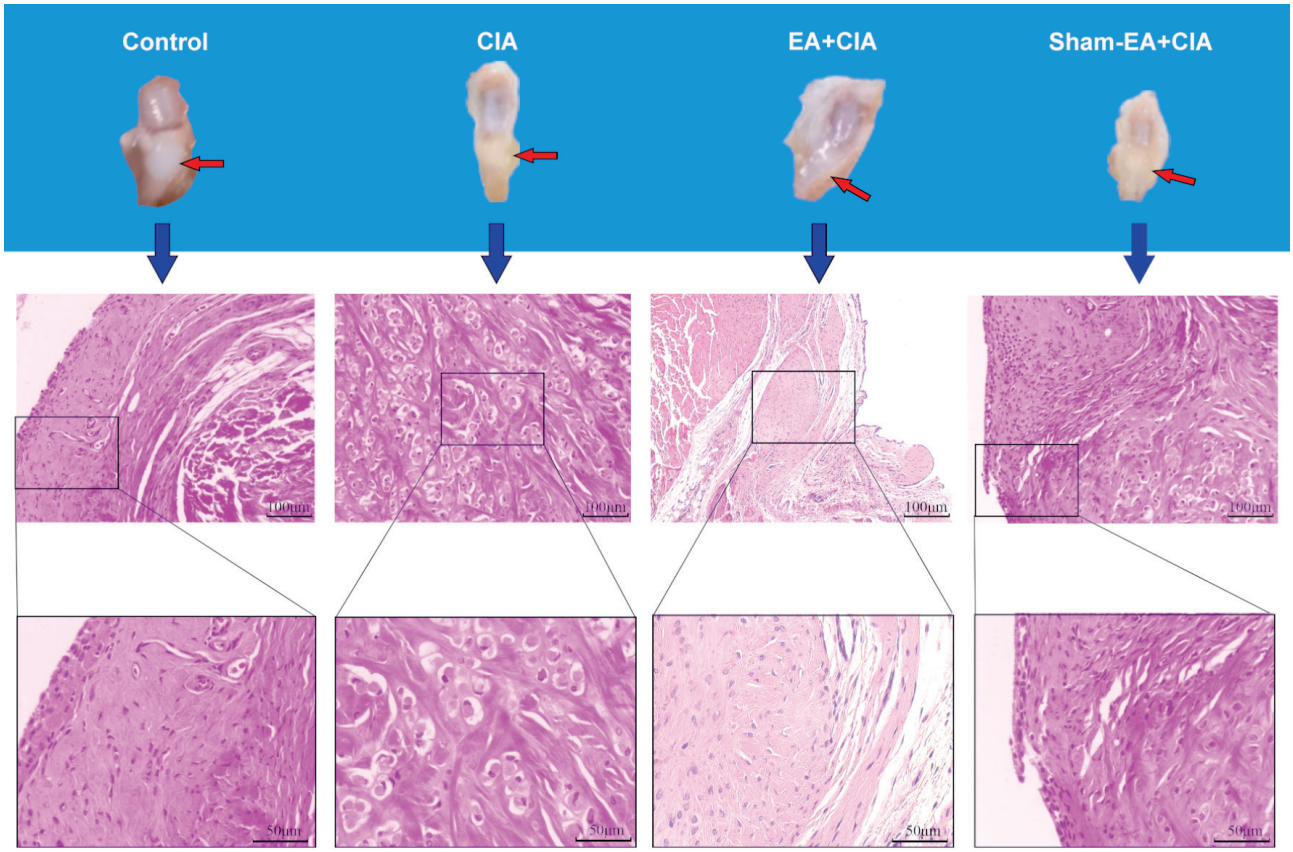

Figure 2. Histological examination of the joint synovium. Representative hematoxylin and eosin (H&E)-stained sections of synovial tissues from control, CIA, EA+CIA, and sham-EA+CIA groups. Red arrows indicate synovial tissue.

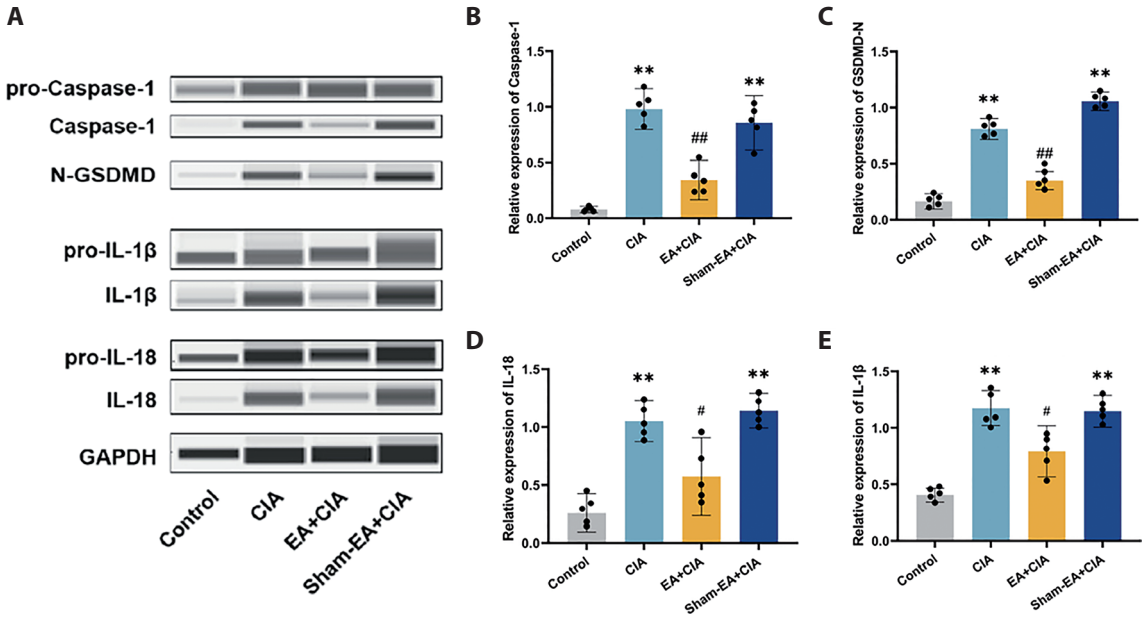

Figure 3. Protein expression of caspase-1–pyroptosis-related markers in synovial tissue. **A.** Representative automated Western blot images of pro-caspase-1, cleaved caspase-1, N-terminal GSDMD (N-GSDMD), pro-IL-1β, mature IL-1β, pro-IL-18, mature IL-18, and GAPDH in each group. **B–E.** Densitometric quantification of cleaved caspase-1, N-GSDMD, IL-1β, and IL-18. For caspase-1, IL-1β, and IL-18, values are expressed as the ratio of mature/precursor forms; N-GSDMD was normalized to GAPDH. Data are presented as mean ± SD. ** $p < 0.01$ *vs.* control; # $p < 0.05$ *vs.* CIA.

Discussion

RA, which is one of the most prevalent chronic inflammatory diseases with an incidence of 0.5% to 1%, carries significant burdens for both individuals and society. Although RA is pathologically heterogeneous, the major clinical characteristic of RA is bone and cartilage lesions caused by osteoclasts that are abnormally activated by a dysfunctional inflammatory response in the synovial compartment (Smolen et al. 2017). Growing evidence shows that pyroptosis is activated in synovial tissues during RA and that inhibiting pyroptosis significantly alleviates joint inflammation and the progression of RA, indicating that pyroptosis is a promising therapeutic target (Wu et al. 2020; Ling et al. 2021; Li W et al. 2022).

Unlike apoptosis, pyroptosis is a proinflammatory PCD triggered by caspases. In the canonical pathway, inflammasomes cleave pro-caspase-1 into a bioactive form. Activated caspase-1 not only cleaves pro-IL-1β and pro-IL-18 into bioactive IL-1β and IL-18, respectively, but also dissociates GSDMD at the Asp275 site to form the C-terminus (C-GSDMD) and N-terminus (N-GSDMD) (Wang et al. 2021; Xia et al. 2021). N-GSDMD migrates and interacts with the cell membrane through lipid binding sites to

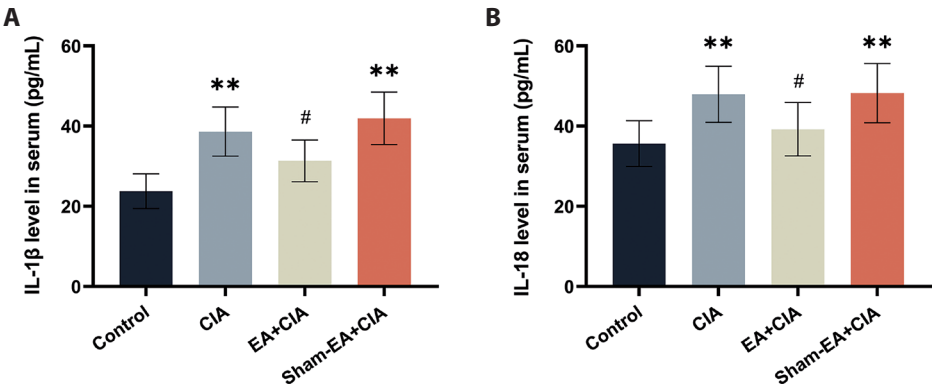

Figure 4. Serum levels of inflammatory cytokines. Serum IL-1β (**A**) and IL-18 (**B**) levels measured on Day 28 by enzyme-linked immunosorbent assay (ELISA). Data are presented as mean ± SD. ** $p < 0.01$ *vs.* control; # $p < 0.05$ *vs.* CIA. CIA, collagen-induced arthritis; EA, electroacupuncture.

perforate the cell membrane and form nonselective pores, which leads to cell swelling and inflammatory cytokine release (He et al. 2015; Liu et al. 2016). Of these cytokines, IL-1β and IL-18 can activate osteoclasts to accelerate bone erosion through the upregulation of RANKL production by T cells in RA synovitis and promote the expression of many other proinflammatory cytokines (Kondo 2021; Levescot et al. 2021). Clinical research demonstrates that the levels of IL-1β and IL-18 in both synovial fluid and peripheral blood are positively correlated with the severity of RA, and high levels of these two cytokines in peripheral blood contribute to other organ diseases, such as interstitial lung disease and depression (Matsuo et al. 2019; Fakra and Marotte 2021). Our data showed that the levels of IL-1β and IL-18 in both synovial tissue and serum were associated with the expression of GSDMD, which further strengthens the concept that the release of IL-18 and IL-1β is an inflammatory hallmark of canonical pyroptosis. However, the levels of caspase-1, GSDMD, IL-1β, and IL-18 in the synovium and IL-1β and IL-18 in peripheral blood were decreased after EA treatment but were not improved in the sham-EA group, suggesting that the anti-inflammatory effect of EA at ST36 is associated with the suppression of caspase-1-mediated pyroptosis.

Acupuncture is a traditional Chinese medicine that has been used for analgesia and anti-inflammatory treatment for thousands of years. EA is an improved form of manual acupuncture (MA) that uses pulsed currents to strengthen the stimulation of acupoints and is widely used in clinical practice. Although MA and EA have similar therapeutic effects in most cases, there is evidence that EA is more effective than MA in clinical treatment of RA (Casimiro et al. 2005). Regarding the mechanism of action, MA can inhibit inflammatory responses by regulating macrophage polarization, whereas EA inhibits inflammatory responses by regulating the T/Th cell balance (Zhu et al. 2015; Yang F. et al. 2021). Our study demonstrated that the inhibition of caspase-1 mediated pyroptosis, which is another important pathway for EA to suppress the inflammatory response in RA. This effect of EA may be related to the vagal–adrenal axis. EA at ST36 increases the secretion of catecholamines, such as dopamine and norepinephrine, by driving the vagal–adrenal axis (Torres-Rosas et al. 2014). A recent study revealed that dopamine suppresses NLRP3 inflammasome activation in nerve cells, which is one of the most important initiators of caspase-1-mediated pyroptosis (Jiang 2023). These studies, together with our findings, may partially explain the mechanism of the anti-inflammatory effect of EA.

Synovium is essential for joint function and structure by supplying nutrients to chondrocytes and preserving various cellular components of the synovial fluid (Zhao 2021). Figure 2 shows that RA rats that received EA had better structural integrity of synovium compared with the nontreatment or placebo treatment groups due to a milder inflammation response. This protective role may contribute to the inhibition of cartilage damage of EA (Shi et al. 2020). In addition to the above findings, Figure 3 showed that, interestingly, activated caspase-1 was decreased while N-GSDMD was increased in the sham-EA group compared with the CIA group. Given that no electrical current was applied in the sham-EA procedure, this discrepancy cannot be attributed to electrostimulation at a non-acupoint. Instead, it may reflect nonspecific procedural stimulation (e.g., shallow needling at a non-acupoint) and/or biological variability. Alternatively, it may suggest a shift toward noncanonical pyroptosis pathways (e.g., caspase-11-related mechanisms) rather than canonical caspase-1–dependent pyroptosis; however, this presumption was not verified in the current study (Ringel-Scaia et al. 2019). On the other hand, the elevated N-GSDMD level inhibited the expression of caspase-1 through a negative feedback mechanism (Chen et al. 2022; Hu et al. 2022). Collectively, these observations raise the possibility that stimulation at an acupoint region versus a non-acupoint may engage different biological responses; however, this presumption was not verified in the current study.

Acupoint localization in rodents inevitably carries spatial uncertainty because external landmarks are less distinct than in humans and different reference atlases may provide slightly different projections. Moreover, the compact anatomy of the rat hindlimb means that a 5-mm separation between the ST36 region and a lateral sham site may not guarantee an inert control, and overlap of receptive fields or spillover via shared neuromuscular and peripheral nerve structures cannot be excluded. Therefore, while our sham procedure (shallow insertion without electrical current) did not reproduce EA-associated improvements, the present design does not allow definitive conclusions regarding strict site specificity. Future work should integrate neuroanatomical validation (e.g., nerve tracing, electrophysiological mapping, or image-guided targeting) and matched-depth/current active-sham or component-resolved designs to rigorously test whether the ST36 region exhibits unique efficacy compared with adjacent sites.

From a translational perspective, these findings also raise an important question: does the observed benefit reflect an acupoint-driven mechanism, or a more generalized regional response to deep-tissue stimulation and neuromodulation? It is therefore important to distinguish between the efficacy of an EA "clinical package" and the necessity of a site-specific, acupoint-dependent mechanism. In the present study, electroacupuncture delivered in the ST36 region under the current parameters improved CIA-associated inflammatory phenotypes and was accompanied by reduced expression of caspase-1/GSDMD/IL-1β/IL-18 in synovial tissue and lower circulating IL-1β/IL-18. However, because our sham control did not match insertion depth and electrical dose,

the current data cannot determine whether these effects are uniquely dependent on ST36 or reflect a more generalized response to deep-tissue electrical stimulation in the region. Clinically, if comparable anti-inflammatory and pyroptosis-modulating effects can be achieved with non–acupoint stimulation using equivalent depth and current, this could potentially simplify implementation toward localized neuromodulation and reduce reliance on acupoint localization. Conversely, if ST36 remains superior under matched-depth/current active-sham validation, this would strengthen the mechanistic basis for acupoint specificity. Therefore, future studies employing matched-depth/current active-sham controls and component-resolved designs are warranted to clarify site-specificity and improve translational scalability.

A major limitation of this study is that the sham-EA procedure differed from EA in three dimensions –needling depth, stimulation site, and electrical current thus serving as a minimal-activation procedural control rather than an "active sham" that isolates a single component. Accordingly, the presumption that the observed effects are acupoint-specific (i.e., uniquely attributable to ST36) was not verified in the current study, and we cannot exclude the possibility that the outcomes reflect a generalized response to deep-tissue electrical stimulation. This is an important limitation, and our future work will incorporate active-sham and component-resolved designs (e.g., matched insertion depth and identical electrical dose at a non-acupoint, and/or factorial designs separating site-, depth-, and current-dependent effects) to rigorously compare acupoints versus non-acupoints and clarify the necessary elements of the intervention. Another limitation is that the effects of EA on upstream inflammasome signaling were not investigated. Several studies have reported that EA can inhibit NLRP3 inflammasome activation; however, the role of the NLRP3 inflammasome in EA treatment of RA remains unclear. Therefore, based on the present findings, systematic mechanistic studies are needed to determine which caspase-1 activator(s) (e.g., specific inflammasome pathways) are involved in EA-associated suppression of synovial pyroptosis.

Conclusion

In this study, we investigated the therapeutic effects of EA delivered at the ST36 region in CIA rat model and examined its association with synovial pyroptosis-related signaling. Under the current stimulation parameters (insertion depth and electrical settings), EA improved arthritis-related inflammatory phenotypes and was accompanied by decreased expression of caspase-1-mediated pyroptosis-related markers in the joint synovium, together with reduced IL-1β and IL-18 levels in both synovium and serum. These findings support EA, as implemented in this protocol, as a potential adjunct neuromodulatory approach to attenuate synovial inflammation and pyroptosis-associated cytokine release in inflammatory arthritis. Nevertheless, due to the present control design, acupoint specificity/necessity and the independent contributions of needling depth versus electrical stimulation cannot be definitively established and require further verification using matched-depth/current active-sham and component-resolved (factorial) experimental designs, ideally complemented by neuroanatomical targeting validation.

Funding. This work was supported by the Zhejiang Provincial Natural Science Foundation of China (LY21H270011) and the Joint TCM Science and Technology Projects of the National Demonstration Zones for Comprehensive TCM Reform (GZY-KJS-ZJ-2025-038).

Ethics approval. This study was approved by the Institutional Research Ethics Committee of The Third Affiliated Hospital of Zhejiang Chinese Medical University (Approval ID: IACUC-20220505-05).

Consent for publication. All authors agreed with the content of the manuscript and approved the final version of the manuscript.

Data availability statement. The datasets used and analyzed during the current study are available from the corresponding author on reasonable request.

Conflicts of interest. The authors report no competing interests in this work.

Contributions of authors. CXL, FK, DZQ writing-original draft, validation, formal analysis, visualization, software, methodology, writing – review & editing; XP conceptualization, data curation, resources, funding acquisition; NXJ conceptualization, data curation; YJB conceptualization, validation, software, methodology, investigation; XYJ conceptualization, software, methodology, investigation.

References

Cai L, Yao ZY, Yang L, Xu XH, Luo M, Dong MM, Zhou GP (2022): Mechanism of electroacupuncture against cerebral ischemia-reperfusion injury: reducing inflammatory response and cell pyroptosis by inhibiting NLRP3 and Caspase-1. Front Mol Neurosci **15,** 822088 https://doi.org/10.3389/fnmol.2022.822088

Casimiro L, Barnsley L, Brosseau L, Milne S, Robinson VA, Tugwell P, Wells G (2005): Acupuncture and electroacupuncture for the treatment of rheumatoid arthritis. Cochrane Database Syst Rev **2005,** CD003788 https://doi.org/10.1002/14651858.CD003788.pub2

Chauhan K, Jandu J, Brent L, Al-Dhahir M (2023): Rheumatoid Arthritis. StatPearls Publishing

Chen Y, Wu L, Shi M, Zeng D, Hu R, Wu X, Han S, He K, Xu H, Shao X, et al. (2022): Electroacupuncture inhibits NLRP3 activation by regulating CMPK2 after spinal cord injury. Front Immunol **13,** 788556

https://doi.org/10.3389/fimmu.2022.788556
Fakra E, Marotte H (2021): Rheumatoid arthritis and depression. Joint Bone Spine **88,** 105200 https://doi.org/10.1016/j.jbspin.2021.105200
Guo C, Fu R, Wang S, Huang Y, Li X, Zhou M, Zhao J, Yang N (2018): NLRP3 inflammasome activation contributes to the pathogenesis of rheumatoid arthritis. Clin Exp Immunol **194,** 231-243 https://doi.org/10.1111/cei.13167
He WT, Wan H, Hu L, Chen P, Wang X, Huang Z, Yang ZH, Zhong CQ, Han J (2015): Gasdermin D is an executor of pyroptosis and required for interleukin-1β secretion. Cell Res **25,** 1285-1298 https://doi.org/10.1038/cr.2015.139
Hu Y, Jiang Y, Li S, Ma X, Chen M, Yang R, Wen S, Moynagh PN, Wang B, Hu G, et al. (2022): The Gasdermin D N-terminal fragment acts as a negative feedback system to inhibit inflammasome-mediated activation of Caspase-1/11. Proc Natl Acad Sci USA **119,** e2210809119 https://doi.org/10.1073/pnas.2210809119
Hyc A, Osiecka-Iwan A, Dziunycz P, Moskalewski S (2007): Preparation of rat synovial membrane for studies of cytokine secretion. Folia Histochem Cytobiol **45,** 57-60
Jiang W, He F, Ding G, Wu J (2023): Dopamine inhibits pyroptosis and attenuates secondary damage after spinal cord injury in female mice. Neurosci Lett **792,** 136935 https://doi.org/10.1016/j.neulet.2022.136935
Kondo N, Kuroda T, Kobayashi D (2021): Cytokine networks in the pathogenesis of rheumatoid arthritis. International journal of molecular sciences. Int J Mol Sci **22,** 10922 https://doi.org/10.3390/ijms222010922
Levescot A, Chang MH, Schnell J, Nelson-Maney N, Yan J, Martínez-Bonet M, Grieshaber-Bouyer R, Lee P Y, Wei K, Blaustein RB, et al. (2021): IL-1β-driven osteoclastogenic Tregs accelerate bone erosion in arthritis. J Clin Invest **131,** e141008 https://doi.org/10.1172/JCI141008
Li W, Wang K, Liu Y, Wu H, He Y, Li C, Wang Q, Su X, Yan S, Su W, et al. (2022): A novel drug combination of mangiferin and cinnamic acid alleviates rheumatoid arthritis by inhibiting TLR4/NFκB/NLRP3 activation-induced pyroptosis. Front Immunol **13,** 912933 https://doi.org/10.3389/fimmu.2022.912933
Li Y, Li Z, He F, Qin C, Fan R, Zhang F, Wang B (2023): Electroacupuncture alleviates cognitive dysfunction and neuronal pyroptosis in septic mice. Acupunct Med **41,** 246-256 https://doi.org/10.1177/09645284221117847
Ling Y, Xiao M, Huang ZW, Xu H, Huang FQ, Ren NN, Chen CM, Lu DM, Yao XM, Xiao LN, et al. (2021): Jinwujiangu capsule treats Fibroblast-Like Synoviocytes of rheumatoid arthritis by inhibiting pyroptosis via the NLRP3/CAPSES/GSDMD pathway. Evid Based Complement Alternat Med **2021,** 4836992 https://doi.org/10.1155/2021/4836992
Liu X, Zhang Z, Ruan J, Pan Y, Magupalli VG, Wu H, et al. (2016): Inflammasome-activated gasdermin D causes pyroptosis by forming membrane pores. Nature **535,** 153-158 https://doi.org/10.1038/nature18629
Lu HL, Chang CM, Hsieh PC, Wang JC, Kung YY (2022): The effects of acupuncture and related techniques on patients with rheumatoid arthritis: A systematic review and meta-analysis. J Chin Med Assoc **85,** 388-400 https://doi.org/10.1097/JCMA.0000000000000659
Matsuo T, Hashimoto M, Ito I, Kubo T, Uozumi R, Furu M, Ito H, Fujii T, Tanaka M, Terao C, et al. (2019): Interleukin-18 is associated with the presence of interstitial lung disease in rheumatoid arthritis: a cross-sectional study. Scand J Rheumatol Suppl **48,** 87-94 https://doi.org/10.1080/03009742.2018.1477989
Ringel-Scaia VM, Beitel-White N, Lorenzo MF, Brock RM, Huie KE, Coutermarsh-Ott S, Eden K, McDaniel DK, Verbridge SS, Rossmeisl JH, et al. (2019): High-frequency irreversible electroporation is an effective tumor ablation strategy that induces immunologic cell death and promotes systemic anti-tumor immunity. EBioMedicine **44,** 112-125 https://doi.org/10.1016/j.ebiom.2019.05.036
Shi J, Gao W, Shao F (2017): Pyroptosis: gasdermin-mediated programmed necrotic cell death. Trends Biochem Sci **42,** 245-254 https://doi.org/10.1016/j.tibs.2016.10.004
Shi X, Yu W, Wang T, Battulga O, Wang C, Shu Q, Yang X, Liu C, Guo C (2020): Electroacupuncture alleviates cartilage degradation: improvement in cartilage biomechanics via pain relief and potentiation of muscle function in a rabbit model of knee osteoarthritis. Biomed Pharmacother **123,** 109724 https://doi.org/10.1016/j.biopha.2019.109724
Smolen JS, Landewé R, Bijlsma J, Burmester G, Chatzidionysiou K, Dougados M, Nam J, Ramiro S, Voshaar M, van Vollenhoven R, et al. (2017): EULAR recommendations for the management of rheumatoid arthritis with synthetic and biological disease-modifying antirheumatic drugs: 2016 update. Ann Rheum Dis **76,** 960-977 https://doi.org/10.1136/annrheumdis-2016-210715
Torres-Rosas R, Yehia G, Peña G, Mishra P, del Rocio Thompson-Bonilla M, Moreno-Eutimio MA, Arriaga-Pizano LA, Isibasi A, Ulloa L (2014): Dopamine mediates vagal modulation of the immune system by electroacupuncture. Nat Med **20,** 291-295 https://doi.org/10.1038/nm.3479
Wan R, Fan Y, Zhao A, Xing Y, Huang X, Zhou L, Wang Y (2022): Comparison of efficacy of acupuncture-related therapy in the treatment of rheumatoid arthritis: a network meta-analysis of randomized controlled trials. Front Immunol **13,** 829409 https://doi.org/10.3389/fimmu.2022.829409
Wang C, Yang T, Xiao J, Xu C, Alippe Y, Sun K, Kanneganti TD, Monahan JB, Abu-Amer Y, Lieberman J, et al. (2021): NLRP3 inflammasome activation triggers gasdermin D-independent inflammation. Sci Immunol **6,** eabj3859 https://doi.org/10.1126/sciimmunol.abj3859
Wang Y, Gehringer R, Mousa SA, Hackel D, Brack A, Rittner HL (2014): CXCL10 controls inflammatory pain via opioid peptide-containing macrophages in electroacupuncture. PloS One **9,** e94696 https://doi.org/10.1371/journal.pone.0094696
Wu XY, Li KT, Yang HX, Yang B, Lu X, Zhao LD, Fei YY, Chen H, Wang L, Li J, et al. (2020): Complement C1q synergizes with PTX3 in promoting NLRP3 inflammasome over-activation and pyroptosis in rheumatoid arthritis. J Autoimmun **106,** 102336 https://doi.org/10.1016/j.jaut.2019.102336

Xia S, Zhang Z, Magupalli VG, Pablo JL, Dong Y, Vora SM, Wang L, Fu TM, Jacobson MP, Greka A, et al. (2021): Gasdermin D pore structure reveals preferential release of mature interleukin-1. Nature **593,** 607-611 https://doi.org/10.1038/s41586-021-03478-3

Xue L, Wang D, Zhang X, Xu S, Zhang N (2020): Targeted and triple therapy-based liposomes for enhanced treatment of rheumatoid arthritis. Int J Pharm **586,** 119642 https://doi.org/10.1016/j.ijpharm.2020.119642

Xue X, Liu X, Pan S, Li J, Wang S, Yuan H, Liu Y, Yue Z (2023): Electroacupuncture treatment of primary dysmenorrhea: a randomized, participant-blinded, sham-controlled clinical trial protocol. Plos One **18,** e0282541 https://doi.org/10.1371/journal.pone.0282541

Yang F, Gong Y, Yu N, Yao L, Zhao X, Hong S, Wang S, Chen B, Xu Y, Pang G, et al. (2021): ST36 acupuncture alleviates the inflammation of adjuvant-induced arthritic rats by targeting monocyte/macrophage modulation. Evid Based Complement Alternat Med **2021,** 9430501 https://doi.org/10.1155/2021/9430501

Yang T, Sun K, Wang C, Swarnkar G, Quan S, Kress D, Xiao J, Alippe Y, Zheng H, Brophy RH, et al. (2021): Gasdermin D deficiency attenuates arthritis induced by traumatic injury but not autoantibody-assembled immune complexes. Arthritis Res Ther **23,** 286 https://doi.org/10.1186/s13075-021-02668-8

Zhao J, Guo S, Schrodi SJ, He D (2021): Molecular and cellular heterogeneity in rheumatoid arthritis: mechanisms and clinical implications. Front Immunol **12,** 790122 https://doi.org/10.3389/fimmu.2021.790122

Zhao J, Jiang P, Guo S, Schrodi SJ, He D (2021): Apoptosis, autophagy, NETosis, necroptosis, and pyroptosis mediated programmed cell death as targets for innovative therapy in rheumatoid arthritis. Front Immunol **12,** 809806 https://doi.org/10.3389/fimmu.2021.809806

Zhou K, Bian C, Gu H, Cheng X, Huang Z, Chen G, Xu J, Yin X (2021): GSDMD-dependent neutrophil extracellular traps formation contributes to fibroblast-like synoviocyte activation in rheumatoid arthritis. Research Square, (preprint) https://doi.org/10.21203/rs.3.rs-401936/v1

Zhu J, Chen XY, Li LB, Yu XT, Zhou Y, Yang WJ, Liu Z, Zhao N, Fu C, Zhang SH, et al. (2015): Electroacupuncture attenuates collagen-induced arthritis in rats through vasoactive intestinal peptide signalling-dependent re-establishment of the regulatory T cell/T-helper 17 cell balance. Acupunct Med **33,** 305-311 https://doi.org/10.1136/acupmed-2014-010732

Received: May 12, 2025
Final version accepted: March 7, 2026